

# Transition Metal Complexes with 2-(*N*-Tosylamino)benzaldehyde 1-Phthalazinylhydrazone

L. D. Popov<sup>a</sup>, I. N. Shcherbakov<sup>a</sup>, S. I. Levchenkov<sup>b,\*</sup>, Yu. P. Tupolova<sup>a</sup>, A. S. Burlov<sup>a</sup>,  
G. G. Aleksandrov<sup>c</sup>, V. V. Lukov<sup>a</sup>, and V. A. Kogan<sup>a</sup>

<sup>a</sup> Southern Federal University, Rostov-on-Don, Russia

<sup>b</sup> Southern Scientific Center, Russian Academy of Sciences, Rostov-on-Don, Russia

<sup>c</sup> Kurnakov Institute of General and Inorganic Chemistry, Russian Academy of Sciences,  
Leninskii pr. 31, Moscow, 119991 Russia

\*e-mail: physchem@yandex.ru

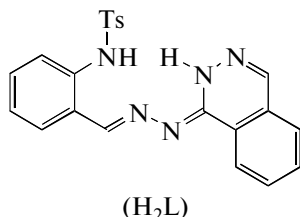
Received August 25, 2010

**Abstract**—2-(*N*-Tosylamino)benzaldehyde 1-phthalazinylhydrazone ( $H_2L$ ) and its complexes with Cu(II), Ni(II), and Mn(II) were obtained. The acid–basic properties of the hydrazone were studied using potentiometry and spectrophotometry. The experimental data were compared with the results of quantum-chemical DFT calculations. The structure of the binuclear complex  $[Cu_2L_2]$  was determined using X-ray diffraction. The broken symmetry approach was used to calculate the exchange coupling constant of the copper ions.

**DOI:** 10.1134/S1070328411060078

Hydrazones and azomethines of polyfunctional carbonyl compounds are ligands under very intensive study in modern coordination and supramolecular chemistry [1–4]. These ligand systems tend to form binuclear complexes with exchange couplings between the metal ions. Such complexes allow relatively easy variation in the electron-donating centers, central ions, and exogenous bridging groups and hence can serve as convenient models for investigation of the main factors that determine the character and strength of exchange couplings between paramagnetic centers; both antiferromagnetic and ferromagnetic exchange is possible [5–9]. Magnetochemical analysis of such exchange-coupled systems is an essential area of coordination chemistry; its ultimate priority is the design of molecular magnetics (these are individual polynuclear complex molecules with high magnetic moments that can retain magnetization [10–15]).

In this work, we studied the physicochemical properties of 2-(*N*-tosylamino)benzaldehyde 1-phthalazinylhydrazone ( $H_2L$ ) and its transition metal complexes.



## EXPERIMENTAL

**Synthesis of  $H_2L$ .** Sodium acetate (0.002 mol) was added to a hot suspension of 1-hydrazinophthalazine hydrochloride (0.002 mol) in ethanol (40 ml). Then a hot solution of 2-(*N*-tosylamino)benzaldehyde (0.002 mol) in ethanol (10 ml) was added. The reaction mixture was refluxed for 4 h and diluted with distilled water (50 ml). The precipitate that formed was filtered off, washed with water, and recrystallized from a mixture of methanol (10 ml) and DMF (4 ml). The yield of  $H_2L$  was 60%.

**Synthesis of transition metal complexes with  $H_2L$  (general procedure).** A hot solution of an appropriate metal salt in methanol was added to a hot solution of  $H_2L$  (0.001 mol) in methanol (20 ml). The reaction mixture was refluxed for 3 h. The precipitate that formed was filtered off, washed with hot methanol, and recrystallized from dioxane or methanol–DMF. The yields of the complexes were 45–70%.

Elemental analysis data and some other characteristics of  $H_2L$ ,  $[Cu_2L_2]$  (I),  $[Cu(HL)(CH_3OH)Cl]$  (II),  $[Cu(HL)(CH_3OH)Br]$  (III),  $[Cu(HL)(CH_3OH)]NO_3$  (IV),  $[Ni(HL)_2]$  (V), and  $[Mn(HL)_2]$  (VI) are given in Table 1.

<sup>1</sup>H NMR spectra were recorded on a Varian Unity 300 spectrometer (300 MHz) in  $DMSO-d_6$  with HMDS as the internal standard; the pulse Fourier mode was used. IR spectra were recorded on a Varian Scimitar 1000 FT-IR instrument in the 400–4000  $cm^{-1}$  range (Nujol). Electronic absorption spectra were recorded on a Varian Cary 50 Scan spectrophotometer. Thermal analysis was carried out on a

**Table 1.** Elemental analysis data for H<sub>2</sub>L and complexes I–VI

| Compound         | Empirical formula  | (Percentage (found/calculated), %) |           |           |           | Color  | <i>T</i> <sub>m</sub> , °C |
|------------------|--|------------------------------------|-----------|-----------|-----------|--------|----------------------------|
|                  |  | C                                  | H         | N         | M         |        |                            |
| H <sub>2</sub> L | C <sub>22</sub> H <sub>19</sub> N <sub>5</sub> O <sub>2</sub> S                  | 62.9/63.3                          | 4.48/4.59 | 16.4/16.8 |           | Yellow | 167                        |
| I                | C <sub>22</sub> H <sub>17</sub> N <sub>5</sub> O <sub>2</sub> SCu                | 55.0/55.2                          | 3.39/3.58 | 14.9/14.6 | 13.0/13.3 | Brown  | >250                       |
| II               | C <sub>23</sub> H <sub>22</sub> ClN <sub>5</sub> O <sub>3</sub> SCu              | 50.1/50.5                          | 3.98/4.05 | 12.5/12.8 | 11.2/11.6 | Brown  | >250                       |
| III              | C <sub>23</sub> H <sub>22</sub> BrN <sub>5</sub> O <sub>3</sub> SCu              | 47.0/46.7                          | 3.84/3.75 | 11.6/11.8 | 10.5/10.7 | Brown  | >250                       |
| IV               | C <sub>23</sub> H <sub>22</sub> N <sub>6</sub> O <sub>6</sub> SCu                | 46.9/48.1                          | 3.99/3.86 | 14.4/14.6 | 11.5/11.1 | Brown  | >250                       |
| V                | C <sub>44</sub> H <sub>36</sub> N <sub>10</sub> O <sub>4</sub> S <sub>2</sub> Ni | 58.8/59.3                          | 4.14/4.07 | 15.2/15.7 | 6.49/6.58 | Brown  | >250                       |
| VI               | C <sub>44</sub> H <sub>36</sub> N <sub>10</sub> O <sub>4</sub> S <sub>2</sub> Mn | 59.7/59.5                          | 3.96/4.09 | 15.5/15.8 | 6.04/6.19 | Yellow | >250                       |

Diamond TG/DTA instrument (Perkin Elmer); samples were heated to 650°C at a rate of 10 K/min. Molar conductivity was determined with a P-38 slidewire bridge for 0.001 M solutions of the complexes in DMF.

**Table 2.** Crystallographic parameters and the data collection and refinement statistics for structure I

| Parameter  | Value  |
|--|--|
| Empirical formula  | C <sub>45</sub> H <sub>37</sub> N <sub>10</sub> O <sub>4.50</sub> S <sub>2</sub> Cu <sub>2</sub> |
| <i>M</i>   | 997.08   |
| Crystal dimensions, mm                                   | 0.32 × 0.12 × 0.12   |
| Temperature, K   | 296(2)   |
| λ, Å   | 0.71073  |
| Crystal system   | Monoclinic   |
| Space group  | <i>C</i> 2/c   |
| <i>a</i> , Å   | 24.583(4)  |
| <i>b</i> , Å   | 11.8898(18)  |
| <i>c</i> , Å   | 17.271(3)  |
| β, deg   | 106.952(4)   |
| <i>V</i> , Å <sup>3</sup>                                | 4828.6(13)   |
| <i>Z</i>   | 4  |
| ρ <sub>calcd</sub> , g/cm <sup>3</sup>                   | 1.372  |
| μ, mm <sup>-1</sup>                                      | 1.042  |
| <i>F</i> (000)   | 2044   |
| 2θ <sub>max</sub> , deg                                  | 50.06  |
| Ranges of <i>h</i> , <i>k</i> , and <i>l</i> indices     | -29 < <i>h</i> < 26<br>-14 < <i>k</i> < 14<br>-20 < <i>l</i> < 20                                |
| Number of measured reflections                           | 13892  |
| Number of independent reflections                        | 4265   |
| Number of parameters refined                             | 300  |
| <i>R</i> <sub>1</sub>                                    | 0.0630   |
| <i>wR</i> <sub>2</sub>                                   | 0.1534   |
| GOOF   | 0.999  |
| Δρ <sub>max</sub> /Δρ <sub>min</sub> , e Å <sup>-3</sup> | 0.717/-0.567   |

Specific magnetic susceptibility was measured using the relative Faraday method in the 77.4–300 K range. The temperature dependence of the magnetic susceptibility of the binuclear complexes was theoretically interpreted in terms of the isotropic-exchange Heisenberg–Dirac–van Vleck model [16, 17].

X-ray diffraction study of complex I was performed on a Bruker Smart CCD Apex II diffractometer (MoK<sub>α</sub> radiation, graphite monochromator). An absorption correction was applied with the SMART program. The structure was solved by the direct method and refined anisotropically (for non-hydrogen atoms) on *F*<sub>hkl</sub><sup>2</sup> by the full-matrix least-squares method. The hydrogen atoms were located geometrically and refined using a riding model (*U*<sub>iso</sub>(H) = *nU*<sub>iso</sub>(C), where *n* = 1.5 for the methyl C atoms and 1.2 for the other C atoms). All calculations were performed with the SHELXL-97 program package [18]. Crystallographic parameters and the data collection and refinement statistics for structure I are summarized in Table 2. Selected bond lengths and bond angles are given in Table 3. The atomic coordinates and thermal parameters have been deposited with the Cambridge Crystallographic Data Collection (no. 787801; deposit@ccdc.cam.ac.uk or <http://www.ccdc.cam.ac.uk>).

Electronic and spatial structures of the complexes were determined using the *ab initio* quantum-chemical DFT calculations (Table 3). For organic compounds, we used the hybrid exchange-correlation functional B3LYP [19] with the Becke exchange functional [20] and the Lee–Yang–Parr correlation functional [21]. The geometries of the complex molecules were preoptimized over all natural variables without symmetry constraints. The minima at the potential energy surface were identified for each structure by calculating a force constant matrix and normal vibrational frequencies. The split-valence basis 6-311G(*d,p*) was used as a basis set. The electronic absorption spectra were calculated in terms of the TDDFT method (B3LYP/6-311G(*d,p*)) [22, 23].

All quantum-chemical calculations were performed with the Gaussian'03 program [24]. For data

**Table 3.** Selected interatomic distances and bond angles in the coordination polyhedra of the copper atoms in structure I

| Distance     | <i>d</i> , Å | Angle          | $\omega$ , deg |
|--------------|--------------|----------------|----------------|
| Cu(1)–Cu(1#) | 3.367(1)     | N(1)Cu(1)N(5)  | 160.8(3)       |
| Cu(1)–N(1)   | 1.934(7)     | N(1)Cu(1)N(2)  | 94.3(3)        |
| Cu(1)–N(5)   | 1.937(8)     | N(5)Cu(1)N(2)  | 78.8(4)        |
| Cu(1)–N(2)   | 1.944(8)     | N(1)Cu(1)N(4#) | 100.7(3)       |
| Cu(1)–N(4#)  | 2.014(8)     | N(5)Cu(1)N(4#) | 95.2(3)        |
|              |              | N(2)Cu(1)N(4#) | 143.5(3)       |

preparation, presentation graphics, and visualization of the calculated results, the ChemCraft program was used [25].

The exchange coupling constant  $2J$  for complex I was calculated according to a tried and tested procedure [26, 27], which is based on the broken symmetry approach proposed by Ginsberg, Noddleman, and Yamaguchi [28, 29] under the assumption of a strong magnetic orbital overlap. The exchange coupling constant is calculated as the difference between the energies of two single-determinant states defined in the context of the infinite Kohn–Sham scheme (BP86/6-311D(*d*) level) [30, 31]: triplet ( $S = 1$ ) and singlet (low spin,  $S = 0$ ). For the latter state, it is assumed that the MO symmetry may be lower than the molecular symmetry (broken symmetry state):

$$2J = \frac{E_{BS}(S=0) - E(S=1)}{1+s^2}, \quad (1)$$

where  $s$  is the overlap integral for the interacting spin MOs;  $s$  is taken to be unity in the limit of large overlap and zero in the limit of small overlap. The triplet-state geometry was optimized over all geometrical parameters without symmetry constraints in the DFT context (BP86/6-311G(*d*)). The energy of the singlet state was calculated using the fixed geometry obtained for the triplet state.

## RESULTS AND DISCUSSION

The structure of H<sub>2</sub>L in solutions and in the solid state was examined by elemental analysis, IR spectroscopy, H<sub>2</sub>L NMR spectroscopy, electronic absorption spectroscopy, and quantum-chemical modeling.

Because of the acidity of the NH protons, the ligand H<sub>2</sub>L can exist as a number of tautomers (Fig. 1, *a*–*c*).

The <sup>1</sup>H NMR spectrum of H<sub>2</sub>L in DMSO-*d*<sub>6</sub> shows signals for the NH protons at  $\delta$  11.8 (s, 1H) and 10.7 ppm (s, 1H); their chemical shifts and disappearance upon the addition of D<sub>2</sub>O suggest the exchange character of both the protons. The spectrum also con-

tains signals at  $\delta$  8.01 (s, 1H, azomethine) and 2.48 ppm (s, 3H, Me). Signals at  $\delta$  8.38 (s, 1H, H(4)) and 8.33 ppm (d, 1H, H(8),  $J = 7.5$  Hz) were assigned to two protons of the phthalazine fragment. The other aromatic protons are manifested as two multiplets at  $\delta$  7.55–7.73 (6H) and 7.09–7.26 ppm (5H).

The IR spectrum of H<sub>2</sub>L shows an absorption band at 1636 cm<sup>-1</sup> (v(C=N)azometh), two bands at 1595 and 1584 cm<sup>-1</sup> (v(C=N)phthal), and two bands at 3440 and 3120 cm<sup>-1</sup> (v(N–H)) (Table 4).

The position of the absorption peak of the phthalazine NH group suggests that H<sub>2</sub>L exists as phthalazone tautomer (*a*), which is also characteristic of other hydrazones derived from hydrazinophthalazine [7, 32, 33].

These data agree with the electronic absorption spectra of H<sub>2</sub>L. The spectral pattern depends on the solvent nature. In ethanol, H<sub>2</sub>L absorbs at 295 and 375 nm. In dioxane and DMF, the longer-wavelength band experiences slight bathochromic shifts by 5 and 10 nm, respectively. In acetone, acetonitrile, and DMSO, the position of this band remains unchanged, while chloroform causes its hypsochromic shift by 15 nm. The position and shape of the shorter-wavelength band are virtually the same in ethanol, dioxane, acetonitrile, and DMF. In chloroform, this band experiences a bathochromic shift by 10 nm.

**Table 4.** IR spectra of H<sub>2</sub>L and complexes I–VI

| Compound         | v(C=N) <sub>azometh</sub> , cm <sup>-1</sup> | v(C=N) <sub>arom</sub> , cm <sup>-1</sup> | v(NH), cm <sup>-1</sup> |
|------------------|--|---|-------------------------|
| H <sub>2</sub> L | 1646   | 1595, 1584                                | 3120, 3440              |
| I                | 1616   | 1592                                      |                         |
| II               | 1620   | 1590                                      | 3171                    |
| III              | 1625   | 1599                                      | 3176                    |
| IV               | 1625   | 1598                                      | 3217                    |
| V                | 1628   | 1597                                      | 3176                    |
| VI               | 1620   | 1595                                      | 3183                    |

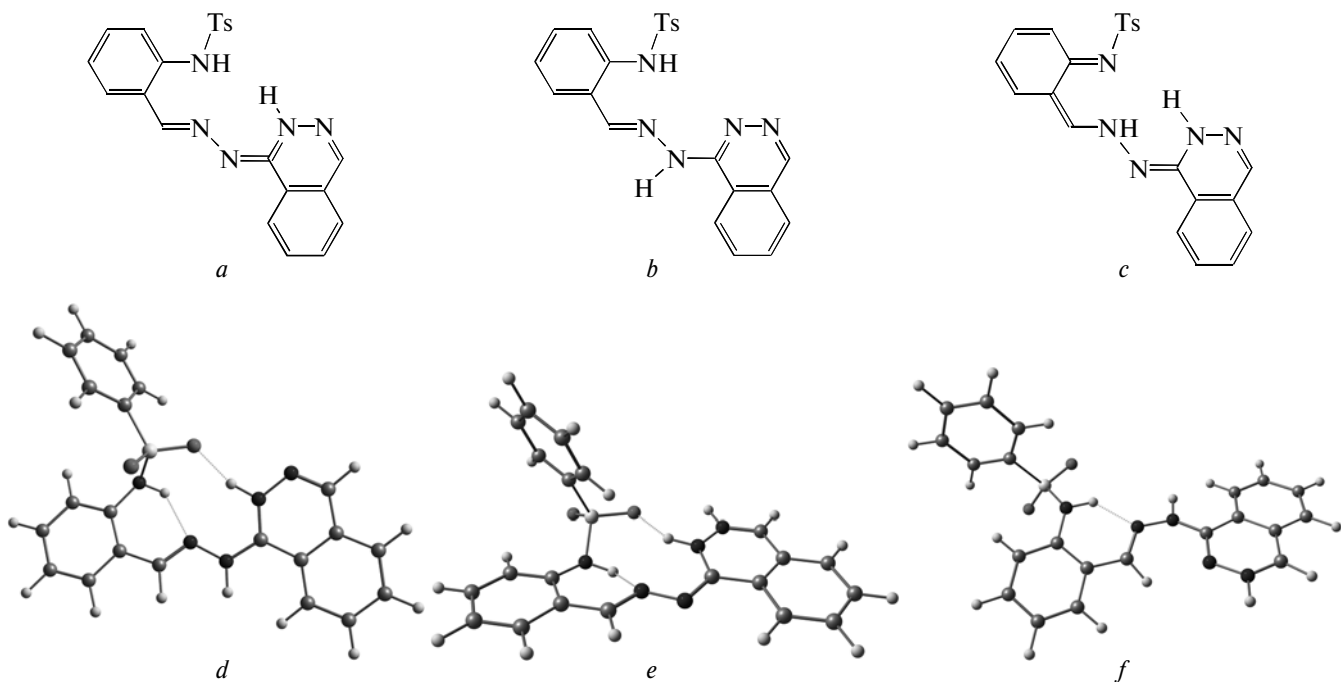


**Fig. 1.** Tautomers (a)–(c) of  $\text{H}_2\text{L}$ . Molecular structure of  $\text{H}_2\text{L}$  and the total energies of its protonated forms:  $-1633.487819$  (d),  $-1633.461955$  (e), and  $-1633.459727$  au (f).

The relative stabilities of tautomers (a)–(c) were calculated using the DFT approach (B3LYP/6-311G(*d,p*)) without and with consideration to the solvent effect in the polarizable continuum model (PCM). The calculated data are given in Table 5. Phthalazone form (a) is much more stable than the two other tautomers in the gas phase and in both solvents; the energy differences between the tautomers in polar (ethanol) and nonpolar solvents (chloroform) are nearly the same. Quinonoid form (c) is somewhat more favorable than amino hydrazone (b) in the gas phase and is considerably stabilized in the polar solvent (ethanol). In chloroform, however, tautomer (c) is the highest-energy structure. Therefore,  $\text{H}_2\text{L}$  exists in solution only as phthalazone tautomer (a).

The protolytic properties of a ligand are crucial for its complexing ability [34–36]. We studied the protolytic equilibria of  $\text{H}_2\text{L}$  in aqueous ethanol using

potentiometry and spectrophotometry. An analysis of the potentiometric titration curve suggests the protonation of the hydrazone molecule; the calculated basicity constant is  $\text{p}K_b = 3.60$ . In the basic range up to pH 12.5, no proton abstraction was detected.

The presence of the sole equilibrium associated with the ligand protonation (cation formation) in the pH range from 2 to 12 was confirmed by spectrophotometric data. In neutral and basic media, the electronic absorption spectra of the solutions are nearly identical; the longer-wavelength band appears at 375 nm. At pH < 3, this band experiences a hypsochromic shift to 355–350 nm. The position of the band at 295 nm is virtually pH-independent.

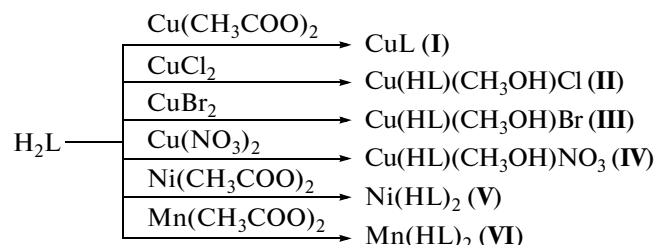
To elucidate the nature of the resulting monocation, we performed quantum-chemical DFT calculations of the structures and total energies of a number of isomeric protonated forms of  $\text{H}_2\text{L}$  (Fig. 1, d–f).

**Table 5.** Calculated total energies  $E$  (au) and relative stabilities  $\Delta E$  (kcal/mol) of the tautomers (a)–(c) of  $\text{H}_2\text{L}$  in the gas phase and in ethanol and chloroform (B3LYP/6-311G(*d,p*), PCM)

| Tautomer | Gas          |            | Ethanol      |            | CHCl <sub>3</sub> |            |
|----------|--------------|------------|--------------|------------|-------------------|------------|
|          | $E$          | $\Delta E$ | $E$          | $\Delta E$ | $E$               | $\Delta E$ |
| a        | -1633.092293 | 0.0        | -1633.109925 | 0.0        | -1633.104875      | 0.0        |
| b        | -1633.073509 | 11.8       | -1633.095433 | 9.1        | -1633.089489      | 9.7        |
| c        | -1633.080041 | 7.7        | -1633.101878 | 5.0        | -1633.087491      | 10.9       |

The hydrazone  $\text{H}_2\text{L}$  is preferentially protonated at the phthalazone N atom (*d*). Structure (*a*) and the presence of monocation (*d*) in solution are confirmed by comparison of the TDDFT-calculated and experimental electronic absorption spectra of these compounds. The calculated wavelengths ( $\lambda$ , nm) and the intensities (oscillator strengths, *f*) of the first five electron transitions are given in Table 6. According to our calculations, tautomer (*a*) absorbs strongly (*f* = 0.5981) at 382 nm, which is close to the observed absorption peak at 375 nm in basic and neutral media. The other transitions in the range up to 320 nm have low intensities. At the same time, monoprotonated form (*d*) should absorb best at 343 nm (*f* = 0.3984), while its absorption at 382 nm is substantially weaker. Thus, the protolytic equilibrium between tautomers (*a*) and (*d*) accurately describes the observed evolution of the electronic absorption spectrum at low pH values.

We obtained a number of transition metal complexes with  $\text{H}_2\text{L}$  using the following reaction scheme:



The molecular formulas and structures of the complexes were determined by elemental analysis, thermogravimetry, IR spectroscopy, conductometry, and magnetochemical measurements.

Reactions of  $\text{H}_2\text{L}$  with cupric acetate, cupric chloride, and cupric bromide gave complexes of the formulas CuL and Cu(HL)(CH<sub>3</sub>OH)X (L<sup>2-</sup> and HL<sup>-</sup> are di- and monodeprotonated forms of H<sub>2</sub>L; X = Cl or Br) (Table 1). According to TG data, the last two complexes contain inner-sphere methanol molecules because the endothermic weight loss at 130–150°C corresponds to one methanol molecule [37, 38].

A reaction of H<sub>2</sub>L with cupric nitrate yielded the complex Cu(HL)(CH<sub>3</sub>OH)NO<sub>3</sub> (**IV**).

Conductometric data for 0.001 M solutions of the complexes in DMF suggest that complex **IV** can be classified among double electrolytes [39] (i.e., the nitrate anion is an outer-sphere ligand in this complex).

According to IR spectra (Table 4), the ligand H<sub>2</sub>L is doubly deprotonated in the complex with cupric acetate and singly deprotonated in the complexes with cupric halides and cupric nitrate. The IR spectra of complexes **II**–**IV** show an absorption band at 3130–3190 cm<sup>-1</sup> (ν(N–H)), which is absent from the IR spectrum of H<sub>2</sub>L. The noticeably changed position of the band ν(N–H)<sub>phthal</sub> in the spectra of the complexes compared to that for the starting hydrazone can be

**Table 6.** Calculated wavelengths  $\lambda$  (nm) and oscillator strengths *f* of the electron transitions for tautomer (*a*) and monocation (*d*)

| Transition | <i>a</i>       |          | <i>d</i>       |          |
|------------|----------------|----------|----------------|----------|
|            | $\lambda$ , nm | <i>f</i> | $\lambda$ , nm | <i>f</i> |
| 1          | 382            | 0.5981   | 378            | 0.1945   |
| 2          | 371            | 0.0882   | 343            | 0.3984   |
| 3          | 346            | 0.0191   | 339            | 0.0109   |
| 4          | 326            | 0.0026   | 326            | 0.0382   |
| 5          | 318            | 0.1067   | 325            | 0.0110   |

explained by the coordination of H<sub>2</sub>L as the hydrazone tautomer. In the IR spectra of all the complexes, the absorption band  $\nu(\text{C}=\text{N})_{\text{azometh}}$  is shifted to 1616–1625 cm<sup>-1</sup>, which provides evidence for the coordination of the azomethine N atom to the copper(II) ion.

The effective magnetic moment  $\mu_{\text{eff}}$  of complex **I** at room temperature (1.23  $\mu_{\text{B}}$ ) is appreciably lower than the spin magnetic moment (1.73  $\mu_{\text{B}}$ ) and decreases to 0.18  $\mu_{\text{B}}$  upon cooling to the boiling temperature of liquid nitrogen (Table 7). These data suggest a very strong antiferromagnetic exchange between the paramagnetic centers in this complex. The exchange coupling constant in complex **I** was calculated in terms of the isotropic-exchange Heisenberg–Dirac–van Vleck model [16, 17] using the Bleaney–Bowers equation [40]:

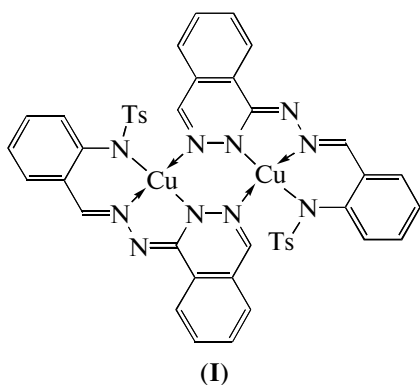
$$\chi'_{\text{M}} = \frac{2N_{\text{A}}g^2\beta^2}{3kT} \times \left[ (1-f) \left[ 1 + \frac{1}{3} \exp\left(\frac{-2J}{kT}\right) \right]^{-1} + fS(S+1) \right] + N_{\alpha}, \quad (2)$$

where  $\chi'_{\text{M}}$  is the diamagnetism-corrected molar magnetic susceptibility,  $N_{\text{A}}$  is Avogadro's number,  $g$  is the Landé factor,  $\beta$  is the Bohr magneton,  $k$  is the Boltzmann constant,  $J$  is the exchange coupling constant,  $f$  is the mole fraction of the paramagnetic impurity, and  $N_{\alpha}$  is the temperature-independent paramagnetism.

The exchange coupling constant  $2J$  is  $-416$  cm<sup>-1</sup> ( $g = 2.20$ ,  $N_{\alpha} = 120 \times 10^{-6}$  cm<sup>3</sup>/mol, and  $f = 0.009$ ). These data provide unambiguous evidence for the dimeric structure of the complex. In this case, dimerization is possible only through the N atoms of the phthalazine fragment: the N atom of the aldehyde fragment can hardly serve as a bridge because of steric hindrances presented by the tosyl group. The  $2J$  value for complex **I** is within the range characteristic of binuclear copper(II) complexes with diazine bridges (from  $-300$  to  $-600$  cm<sup>-1</sup> [7, 41, 42]).

**Table 7.** Magnetic properties of complexes **I–VI** and the molar conductivities of their 0.001 M solutions in DMF

| Complex    | T, K | $\mu_{\text{eff}}$ , $\mu B$ | $2J$ , $\text{cm}^{-1}$ | $\lambda$ , $\Omega^{-1} \text{cm}^2 \text{mol}^{-1}$ |
|------------|------|------------------------------|-------------------------|---|
| <b>I</b>   | 293  | 1.23                         | −416                    | 9.3   |
|            | 77.4 | 0.18                         |                         |   |
| <b>II</b>  | 293  | 2.02                         | 10                      | 11  |
|            | 77.4 | 1.88                         |                         |   |
| <b>III</b> | 293  | 2.12                         | 55                      | 11  |
|            | 77.4 | 2.03                         |                         |   |
| <b>IV</b>  | 293  | 1.81                         | 11                      | 12  |
|            | 77.4 | 1.79                         |                         |   |
| <b>V</b>   | 293  | 2.93                         | 5.95                    | 11  |
|            | 77.4 | 2.87                         |                         |   |
| <b>VI</b>  | 293  | 5.95                         | 5.87                    | 12  |
|            | 77.4 | 5.87                         |                         |   |



Structure **I** determined from spectroscopic and magnetochemical measurements was confirmed by X-ray diffraction. The complex crystallizes as a 2 : 1 solvate with a disordered DMSO molecule. Since the complex molecule has a symmetry axis  $C_2$  passing through the midpoint of the Cu–Cu distance, two mononuclear fragments CuL are fully identical. For designation of symmetry-related atoms, we simply add the character # (the molecular structure of complex **I** with atomic numbering is shown in Fig. 2). Crystallographic parameters of structure **I** are given in Table 2. Selected bond lengths and bond angles are given in Table 3.

In the binuclear complex, the copper ion is pentacoordinated. The coordination sphere of Cu includes three N atoms of one ligand ( $\text{Cu}(1)-\text{N}(1)$ , 1.934(7) Å;  $\text{Cu}(1)-\text{N}(2)$ , 1.944(8) Å; and  $\text{Cu}(1)-\text{N}(5)$ , 1.937(8) Å) and the N(4#) atom of the second ligand at a noticeably longer distance from the copper ion ( $\text{Cu}(1)-\text{N}(4#)$ , 2.014(8) Å). The mononuclear fragments dimerize through this atom to form the six-membered exchange ring  $\text{Cu}(1)-\text{N}(5)-\text{N}(4)-\text{Cu}(1#)-\text{N}(5#)-\text{N}(4#)$ . The coordination sphere is completed by the tosyl O(2) atom ( $\text{Cu}(1)-\text{O}(2)$ , 2.774(7) Å), giving a strongly distorted trigonal bipyramidal geometry.

amid with the axial N(1) and N(5) atoms ( $\text{N}(1)\text{Cu}(1)\text{N}(5)$ , 160.9(3)°) and the equatorial N(2), N(4#), and O(2) atoms. Although the Cu(1)–O(2) bond is long, these atoms interact greatly, which is evident from the virtually planar fragment Cu(1)–O(2)–S(1)–N(1) (the deviations of the atoms are  $\pm 0.002$  Å). The five-membered chelate ring has an envelope conformation with the copper atom as a flap projecting out of the mean-square plane of the other four atoms by 0.171(1) Å. The six-membered chelate ring is distorted much more strongly because of inflections along the lines N(1)–C(7) and N(1)–N(2). The structures of the monomeric complex fragments are nearly planar (except for the tosyl fragments in the flagpole position with respect to the ligand plane). The aromatic rings of the phthalazine and benzaldehyde fragments are virtually coplanar, making an angle of 1.5°. The Cu atom deviates from this plane by 0.294(1) Å. The dihedral angle between the planes of two monomeric fragments is 64.4°.

As a result, in contrast to documented complexes with phthalazine bridges [7], the six-membered exchange fragment in complex **I** is noticeably nonplanar and has a boat-like conformation with apical copper atoms. This is due to steric repulsion between the tosylaminobenzaldehyde fragment of one ligand and the phthalazine fragment of the other ligand. The copper atoms are spaced at 3.367(1) Å. Note that for the binuclear copper(II) complex with 2-acetylbenzimidazole 1-phthalazinylhydrazone, in which steric hindrances are less substantial, quantum-chemical calculations lead to a similar structure for the exchange fragment [27].

Because of steric repulsion, the phenyl rings of the tosyl fragments in structure **I** are virtually parallel to each other, their planes making a dihedral angle of ~9°.

The great exchange integral for complex **I**, despite the long distance between the copper ions and the

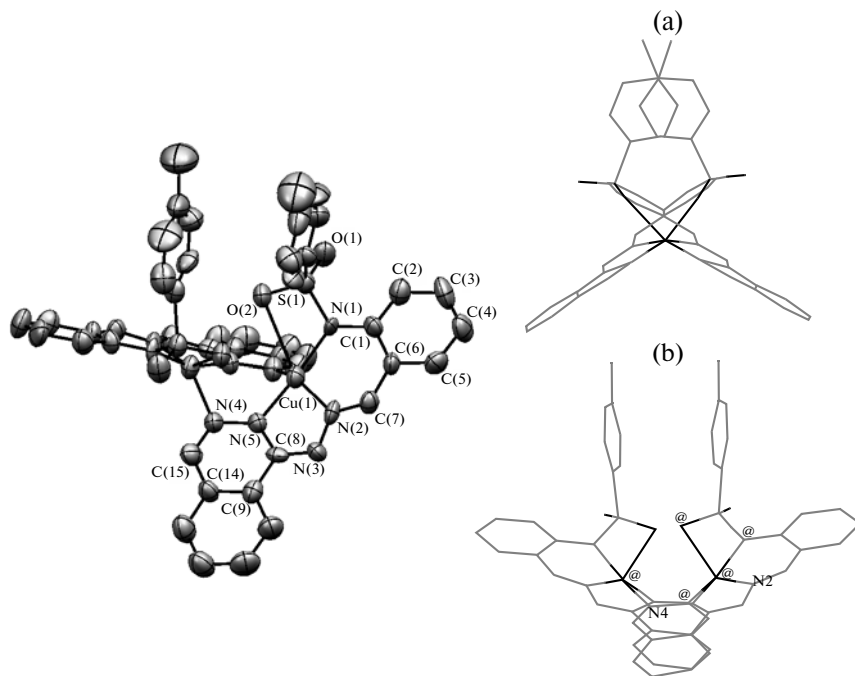


**Fig. 2.** Structure I with atomic thermal displacement ellipsoids (50% probability); the hydrogen atoms are omitted. The projections (a) along and (b) normally to the line Cu–Cu.

nonplanar structure of the exchange fragment, can be attributed to considerable delocalization of the magnetic orbitals over the N atoms of the phthalazine bridges and the interacting copper atoms.

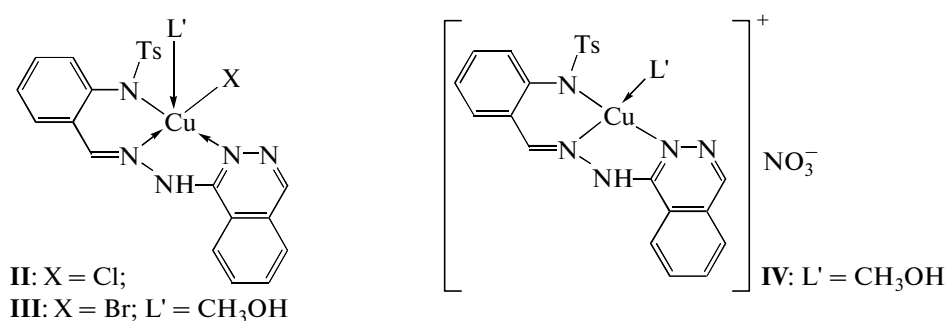
We performed quantum-chemical modeling of exchange couplings in complex I in the context of the broken symmetry approach. We found that the total energies and squared spin moments are  $-6545.352311$  au and  $2.0032$  for the high-spin (HS) state and  $-6545.356476$  au and  $0.7372$  for the low-spin (LS) state, respectively. The exchange coupling constant calculated by formula (1) in the limit of strong overlap is  $457\text{ cm}^{-1}$ .

Both the spin MOs are substantially delocalized over the exchange fragment (Fig. 3). Either MO is considerably contributed by the  $d_{\sigma}$ -AOs of both copper atoms and the  $\sigma$ -AOs of the bridging N atoms of the phthalazine fragment. This validates the use of the large overlap limit ( $s = 1$  in formula (1)). The antiferromagnetic exchange coupling constant calculated

in this approximation ( $-457\text{ cm}^{-1}$ ) is in satisfactory agreement with the experimental value ( $2J = -416\text{ cm}^{-1}$ ).

The unpaired electrons are largely delocalized over the electron-donating atoms of the ligand in both the triplet and low-spin states (Table 8). Near either Cu atom, the spin density sign on all electron-donating atoms in the low-spin state is the same as on the metal ion; the spin density sign in the exchange fragment is reversed between the phthalazine N atoms, which accounts for the considerable antiferromagnetic exchange in this complex.

The effective magnetic moments of complexes II–IV are close to the spin magnetic moments for the  $\text{Cu}^{2+}$  ion and remain virtually unchanged upon cooling (Table 7). The absence of exchange couplings between the  $\text{Cu}^{2+}$  ions in combination with other physico-chemical data allows, with a high probability, their structures to be represented as the following monomers:



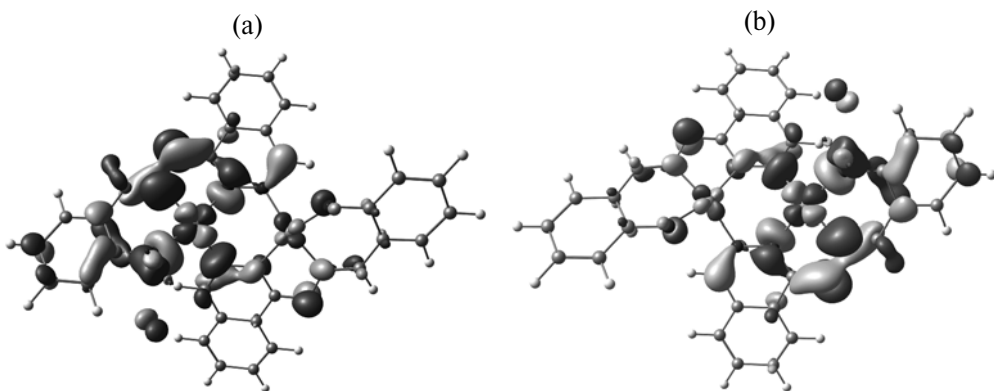


**Fig. 3.** Magnetic spin orbitals of the electrons with the  $\alpha$ - and  $\beta$ -orientations of the spin in the low-spin state: (a)  $237\alpha$  (HOMO),  $E = -0.1689$ ; (b)  $237\beta$  (HOMO),  $E = -0.1689$ . The atoms of the tosyl fragments are omitted; their AOs are virtually not involved in these spin MOs.

Reactions of  $\text{H}_2\text{L}$  with nickel(II) acetate and manganese(II) acetate gave the complexes **V** and **VI** ( $\text{HL}^-$  is a monodeprotonated  $\text{H}_2\text{L}$ ; Table 1). The IR spectra of complexes **V** and **VI** show an absorption band at  $\sim 3200 \text{ cm}^{-1}$  (NH stretching vibrations in the hydrazinophthalazine fragment). The band  $\nu(\text{C}=\text{N})_{\text{azometh}}$  in their spectra is shifted to  $1620$ – $1628 \text{ cm}^{-1}$ .

The  $\mu_{\text{eff}}$  values of complexes **V** and **VI** at room temperature are  $2.93$  and  $5.95 \mu_{\text{B}}$ , respectively; on cooling, they remain virtually unchanged (Table 7). Hence, complexes **V** and **VI** can be represented as mononuclear octahedral structures.

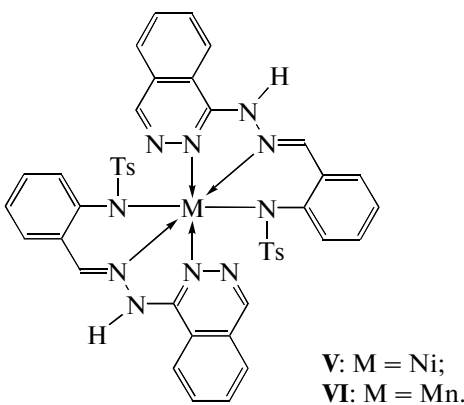


**Table 8.** Mulliken spin density population (au) of the atoms in the exchange fragment of the HS ( $S = 1$ ) and LS states of complex **I**

| Atom  | LS          | HS, $S = 1$ |
|-------|-------------|-------------|
| Cu(1) | $\pm 0.430$ | 0.494       |
| N(5)  | $\pm 0.078$ | 0.092       |
| N(4#) | $\pm 0.049$ | 0.057       |
| N(1)  | $\pm 0.072$ | 0.084       |
| N(2)  | $\pm 0.111$ | 0.129       |

## ACKNOWLEDGMENTS

This work was supported by the Federal Target Program “Scientific and Pedagogical Personnel of the Innovative Russia” (State Contract no. 02.740.11.0255).

## REFERENCES

- Popov, L.D., Shcherbakov, I.N., Tupolova, Yu.P., et al., *Usp. Khim.*, 2009, vol. 78, no. 7, p. 697.
- Alexeev, Yu.E., Kharisov, B.I., Hernandez Garcia, T.C., and Garnovskii, A.D., *Coord. Chem. Rev.*, 2010, vol. 254, nos. 7–8, p. 794.
- Lobana, T.S., Sharma, R., Bawa, G., and Khanna, S., *Coord. Chem. Rev.*, 2009, vol. 253, nos. 7–8, p. 977.
- Stadler, A.-M. and Harrowfield, J., *Inorg. Chim. Acta*, 2009, vol. 362, no. 12, p. 4298.
- Kogan, V.A. and Lukov, V.V., *Koord. Khim.*, 2010, vol. 36, no. 6, p. 401 [*Russ. J. Coord. Chem.* (Engl. Transl.), vol. 36, no. 6, p. 401].
- Starikov, A.G., Kogan, V.A., Lukov, V.V., et al., *Koord. Khim.*, 2009, vol. 35, no. 8, p. 625 [*Russ. J. Coord. Chem.* (Engl. Transl.), vol. 35, no. 8, p. 616].
- Kogan, V.A., Levchenkov, S.I., Popov, L.D., and Shcherbakov, I.N., *Ross. Khim. Zh.*, 2009, vol. 53, no. 1, p. 86.
- Uraev, A.I., Vasilchenko, I.S., Ikorskii, V.N., et al., *Mendeleev Commun.*, 2005, vol. 15, no. 4, p. 133.
- Burlov, A.S., Ikorskii, V.N., Nikolaevskii, S.A., et al., *Zh. Neorg. Khim.*, 2008, vol. 53, no. 10, p. 1677 [*Russ. J. Inorg. Chem.* (Engl. Transl.), vol. 53, no. 10, p. 1566].
- Ovcharenko, V.I. and Sagdeev, R.Z., *Usp. Khim.*, 1999, vol. 68, no. 6, p. 381.
- Kahn, O., *Acc. Chem. Res.*, 2000, vol. 33, no. 10, p. 647.
- Leuenberger, M.N. and Loss, D., *Nature*, 2001, vol. 410, p. 789.
- Kalinikov, V.T., Rakitin, Yu.I., and Novotortsev, V.M., *Usp. Khim.*, 2003, vol. 72, no. 11, p. 1123.
- Gatteschi, D. and Sessoli, R., *Angew. Chem., Int. Ed. Engl.*, 2003, vol. 42, p. 268.
- Mrozniski, J., *Coord. Chem. Rev.*, 2005, vol. 249, p. 2534.

16. Rakitin, Yu.V. and Kalinnikov, V.T., *Sovremennaya magnetokhimiya* (Modern Magnetochemistry), St. Petersburg: Nauka, 1994.
17. Rakitin, Yu.V., *Itogi Nauki Tekh. Stroenie Molekul i Khimicheskaya Svyaz'*, Moscow: VINITI, 1986, vol. 10, p. 132.
18. Sheldrick, G.M., *Acta Crystallogr., Sect. A: Found. Crystallogr.*, 2008, vol. 64, no. 1, p. 112.
19. Stephens, P.J., Devlin, F.J., Chabalowski, C.F., and Frisch, M.J., *J. Phys. Chem.*, 1994, vol. 98, no. 45, p. 11623.
20. Becke, A.D., *J. Chem. Phys.*, 1993, vol. 98, no. 7, p. 5648.
21. Lee, C., Yang, W., and Parr, R.G., *Phys. Rev. B: Condens. Matter.*, 1988, vol. 37, no. 2, p. 785.
22. Stratmann, R.E., Scuseria, G.E., and Frisch, M.J., *J. Chem. Phys.*, 1998, vol. 109, no. 19, p. 8218.
23. Bauernschmitt, R. and Ahlrichs, R., *Chem. Phys. Lett.*, 1996, vol. 256, nos. 4-5, p. 454.
24. Frisch, M.J., Trucks, G.W., Schlegel, H.B., et al., *Gaussian 03, Revision D.01*, Wallingford (CT, USA): Gaussian, Inc., 2004.
25. Popov, L.D., Shcherbakov, I.N., Levchenkov, S.I., et al., *J. Coord. Chem.*, 2008, vol. 61, no. 3, p. 392.
26. Popov, L.D., Levchenkov, S.I., Shcherbakov, I.N., et al., *Zh. Obshch. Khim.*, 2010, vol. 80, no. 12, p. 2040 [*Russ. J. Gen. Chem. (Engl. Transl.)*, vol. 80, no. 12, p. 2501].
27. Ginsberg, A.P., *J. Am. Chem. Soc.*, 1980, vol. 102, no. 1, p. 111.
28. Noddeman, L., Peng, C.Y., Case, D.A., and Mouesca, J.-M., *Coord. Chem. Rev.*, 1995, vol. 144, p. 119.
29. Becke, A.D., *Phys. Rev. A: Gen. Phys.*, 1988, vol. 38, no. 6, p. 3098.
30. Perdew, J.P., *Phys. Rev. B: Condens. Matter*, 1986, vol. 33, no. 12, p. 8822.
31. Paolucci, G., Stelluto, S., Sitran, S., et al., *Inorg. Chim. Acta*, 1992, vol. 193, no. 1, p. 57.
32. Giorgi, G., Ponticelli, F., Savini, L., et al., *J. Chem. Soc., Perkin Trans.*, 2000, p. 2259.
33. Shoukry, A.A. and Shoukry, M.M., *Spectrochim. Acta, Part A*, 2008, vol. 70, no. 3, p. 686.
34. Popov, L.D., Askalepova, O.I., Levchenkov, S.I., and Kogan, V.A., *Zh. Neorg. Khim.*, 2007, vol. 52, no. 4, p. 686 [*Russ. J. Inorg. Chem. (Engl. Transl.)*, vol. 52, no. 4, p. 626].
35. Popov, L.D., Levchenkov, S.I., Shcherbakov, I.N., and Kogan, V.A., *Zh. Obshch. Khim.*, 2007, vol. 77, no. 7, p. 1203 [*Russ. J. Gen. Chem. (Engl. Transl.)*, vol. 77, no. 7, p. 1284].
36. Kukushkin, Yu.N., Khodzhaev, O.F., and Baranova, V.F., *Termoliz Koordinatsionnykh Soedinenii* (Thermolysis of Coordination Compounds), Tashkent: Fan, 1986.
37. Samus', N.M., Tsapkov, V.I., and Kravchenko, V.N., *Zh. Obshch. Khim.*, 1997, vol. 67, no. 12, p. 2044 [*Russ. J. Gen. Chem. (Engl. Transl.)*, vol. 67, no. 12, 1929].
38. Geary, W.J., *Coord. Chem. Rev.*, 1971, vol. 7, no. 1, p. 81.
39. Bleaney, B. and Bowers, K.D., *Proc. R. Soc. London: A*, 1952, vol. 214.
40. Tandon, S.S., Thompson, L.K., and Hynes, R.C., *Inorg. Chem.*, 1992, vol. 31, no. 11, p. 2210.
41. Abraham, F., Lagrenée, M., Sueur, S., et al., *Dalton Trans.*, 1991, p. 1443.